

Key words: *squat-type crack, crack in rail treads, rail-wheel contact, dynamic contact force, railway bogie-truck system*

MIROSLAW OLZAK^{*)}, TOMASZ SZOLC^{**)}

DYNAMICS EFFECTS CAUSED BY THE “SQUAT” TYPE OF A CRACK IN THE RAIL TREADS

The authors present the part of research devoted to the “squat”-type crack development in the heads of railway rails. This paper contains description of the results of investigations of the influence of the dynamic interaction, between the railway bogie running along the track on the “squat”-type crack development. The studies are performed by the use of computer simulation technique. The study is divided into two parts. The first part explains, how the vertical displacement of the wheel varies during the quasi-static rolling of the bogie wheel along the cracked rail. In the second part of the paper, this displacements fluctuation is introduced to dynamic analysis. The histories of the wheel-rail force fluctuation during passage along the rail with the “squat”-type crack were obtained as the result of dynamic analysis.

NOMENCLATURE

- a – length of crack
 E – Young’s modulus
 C – damping-gyroscopic matrix,
 F – external excitation vector,
 K – stiffness matrix,
 K_I, K_{II} – mode I and II stress intensity factors
 l_s – sleeper spacing,
 M – mass matrix.

^{*)} *Institute of Aeronautics and Applied Mechanics, Warsaw University of Technology, ul. Nowowiejska 24, 00-665 Warsaw, Poland; E-mail: zpk-mo@meil.pw.edu.pl*

^{**)} *Institute of Fundamental Technological Research of the Polish Academy of Sciences, ul. Świętokrzyska 21, 00-049 Warsaw, Poland; E-mail: tszolc@ippt.gov.pl*

n	– index,
p_n, t_x	– normal and tangential force in nodes being in contact
$r_n(t)$	– Lagrange’s co-ordinate,
$\mathbf{r}(t)$	– Lagrange’s co-ordinate vector,
Q	– normal load
t	– time,
α	– inclination angle of crack
ΔK	– range of the SIF fluctuation
Δz	– vertical displacement of the center of the cylinder
ν	– Poisson’s ratio
v_0	– train travelling speed,

1. Introduction

In the paper, the authors investigate the “squat”-type cracks in the rail treads. Cracks of this type quite frequently occur in rails of the railway tracks characterized by the combined passenger and freight traffic. An explanation of the most significant factors influencing a development of these cracks is the main purpose of investigations. Till present, according to the references [1], [2], [3], [4], [5] the following factors that influence the “squat”-type crack development have been subject of studies: crack dimensions, crack inclination angle, coefficient of friction between the crack walls, internal stresses in rails, thermal stresses, rail traction loads caused by braking and acceleration of the railway vehicles, various models of interaction between the crack walls, degradation of mechanical properties of the layers covering the crack faces, gap between the crack faces and others.

In this paper, the investigations are focused on the influence of dynamic load on the “squat”-type crack development. The loaded railway wheel rolling along the rail tread slightly subsides on the cracks, which induces dynamic wheel-rail contact forces. The main problems to explain are: how strong are these forces and does their action cause the “squat”-type crack development. In order to answer these questions, in the first step the vertical displacement of the wheel during run along the crack was estimated. Then, these displacements were assumed as the kinematic external excitations for the dynamic analysis of the railway bogie interacting with the track. By means of numerical simulation for the freight car bogie running along the cracked rail, the time histories of the dynamic wheel-rail contact forces were obtained. The conclusions about the influence of dynamic load on the “squat”-type crack development were drawn on the basis of the comparison the wheel-rail contact force fluctuation and the respective variations of the stress intensity factors.

2. Part I – Determination of the vertical displacement of the railway wheel

The "squat"-type cracks occur in the rail head. They are characterized by a complicated spatial shape. In the initial stage of development, their shape is close to half-elliptical with the main axis inclined under the angle of 45 degrees with regard of the rail longitudinal symmetry plane and with the crack plane inclined under the angle within the range of $15 \div 20^\circ$ degrees with regard to the horizontal plane. However, for determination of the railway wheel vertical displacements, the 2-dimensional contact analysis was applied in order to avoid complications associated with an application of the 3-dimensional contact analysis. The representation of the "squat"-type crack in the 2D-model is presented in Fig. 1.

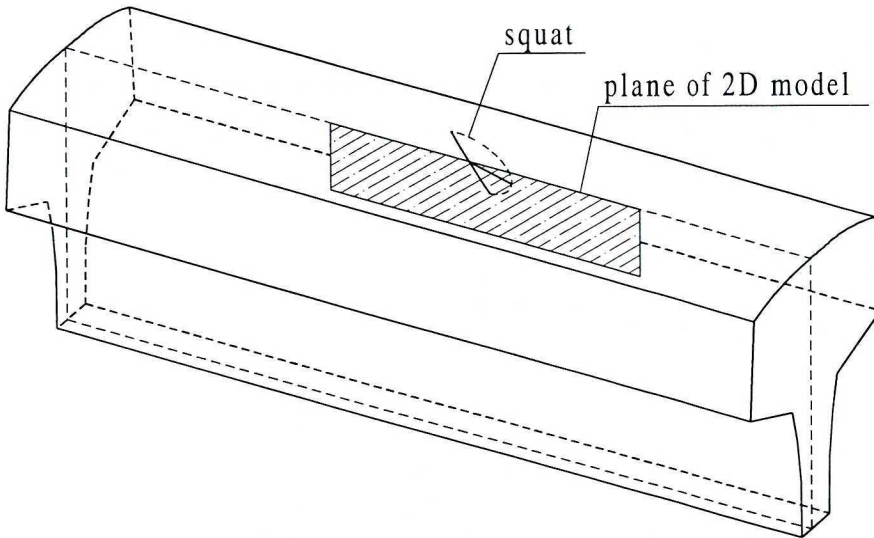


Fig. 1. The "squat"-type crack in the rail tread and its representation in the rail 2D-model

Such simplification leads to a greater variation of the wheel vertical displacements, because the results determined using this approach correspond to the whole rail head, cracked as shown in Fig. 2.

Similarly, at further stages of the research, the authors consequently took assumptions aiming at emphasizing the influence of the crack on dynamic effects.

The 2-dimensional model consists of the rectangular prism with the oblique crack as well as of the cylinder with a diameter equal to the railway wheel diameter. The support of the prism and its dimensions are presented in Fig. 3.

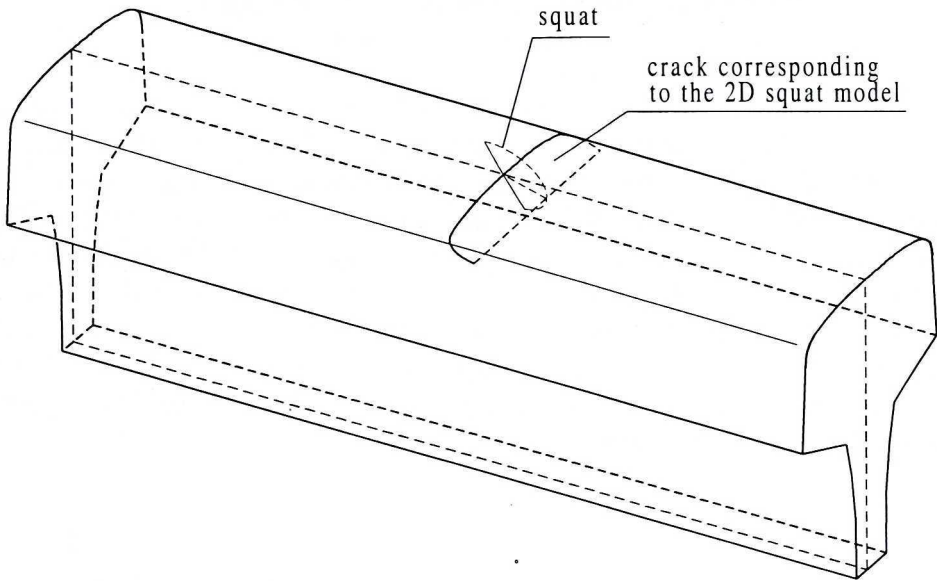


Fig. 2. Interpretation of the half-elliptical "squat"-type crack for analysis using the 2D model

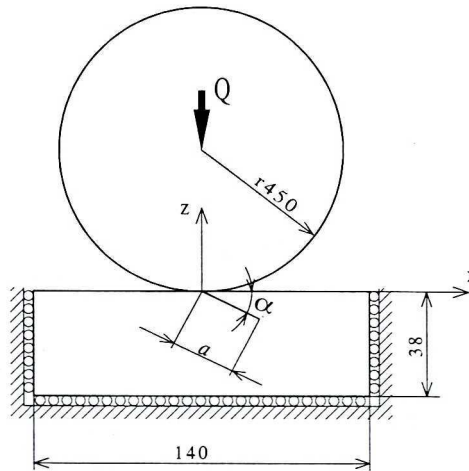


Fig. 3. Scheme of the 2-D cracked rail model with the railway wheel

The length of the crack and its inclination angle were equal $a = 20.3$ mm and $\alpha = 25$ deg, respectively. The value of static load was selected in order to obtain maximal pressure on the contact area reaching ca. 900 MPa, which corresponded to the realistic wheel-rail pressure value for the common railway freight car axle loading 230 kN. For the assumed plane state of strain, the cylinder load was equal to 9 kN/mm. The same mechanical properties

were assumed for the material of the prism and cylinder, which corresponded to the properties of steel, i.e. $E = 210000$ MPa and $\nu = 0.3$. The linear-elastic material was assumed in the analysis. The analysis was quasi-static in character. The two investigated variants of the crack were without and with the gap between the crack faces, respectively.

In the second case, for the unloaded state, the gap between the faces varied linearly from $15 \mu\text{m}$ at the surface to 0 at the tip of the crack. Such gap was selected to represent the crack wall wear observed in real cracks of the rails.

The Coulomb model of friction was applied between the prism and the cylinder with the coefficient $\mu_p = 0.4$. However, no friction was assumed between the crack faces, i.e. $\mu_s = 0$, in order to maximize the vertical displacements of the cylinder caused by the crack.

In order to solve the contact problem between the prism and the cylinder as well as between the crack faces the authors used the method based on applying flexibility matrices of the bodies in contact [6]. The standard finite element code was applied to determine the flexibility matrices. An appropriate boundary element, finite difference codes or other analytical-numerical methods could be used for this purpose, because the flexibility matrix method does not requires any contact elements.

The numerical simulation of the process of cylinder rolling along the prism consisted of many partial solutions of the contact problem for the successive cylinder positions. In the each solution, the final state of the former solution was assumed as the initial state during the simulation. Normal and tangential forces in the mesh nodes belonging to the contact were determined. One also found the micro-slip in such nodes where the following condition was not satisfied:

$$t_x \leq p_n \cdot \mu \quad (1)$$

where p_n , t_x are the normal and tangential force, respectively, and μ denotes the coefficient of friction.

Each solution was used to determine the vertical displacement Δz of the cylinder's center necessary to reduce to zero the clearance between the cylinder and the prism, so that the two surfaces, deflecting under the contact forces, would touch one another.

The results of these solutions were stored for each 0.125 mm to be used for drawing diagrams presented below. The contact forces determined from the solution of the contact problem were applied to calculate the stresses and displacement in the prism, and then these stresses and displacements were used for determination of the stress intensity factors at the tip of the crack.

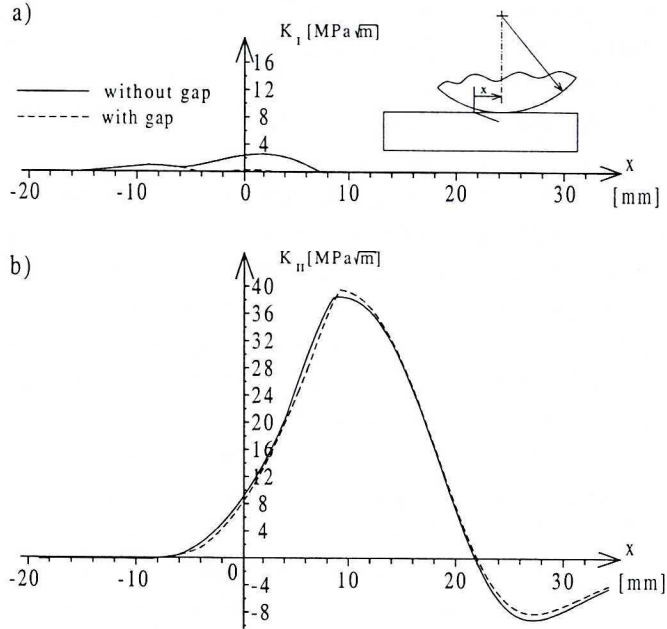


Fig. 4. Histories of the stress intensity factors during quasi-static rolling of the cylinder along the cracked prism

Figure 4 presents the variation histories of the Stress Intensity Factors during quasi-static rolling of the cylinder along the cracked prism. The origin of x -co-ordinate is set at the crossing point of the crack edge with the prism surface. Two diagrams correspond to the crack with and without the gap.

If the amplitudes ΔK_I and ΔK_{II} of the Stress Intensity Factors significantly increase in comparison with those shown in Fig. 4 because the dynamic phenomena are taken into consideration. It means that the dynamic loads can play a significant role during the “squat”-type crack development in the rails. It is to emphasize that in such conditions the development of these cracks is possible but not very probable because the way of modeling as well as the selected parameters for simulation have been assumed in order to maximize severity of the phenomena associated with the crack presence in the rail tread.

The vertical displacement of the center of the cylinder Δz for the successive cylinder positions was used for drawing the diagram presented in Fig. 5. It follows from this figure that rolling of the cylinder along the crack with a gap yields greater displacement values Δz , i.e. deeper jumps down of the cylinder during run along the cracked prism with a gap, which results in stronger dynamic effects.

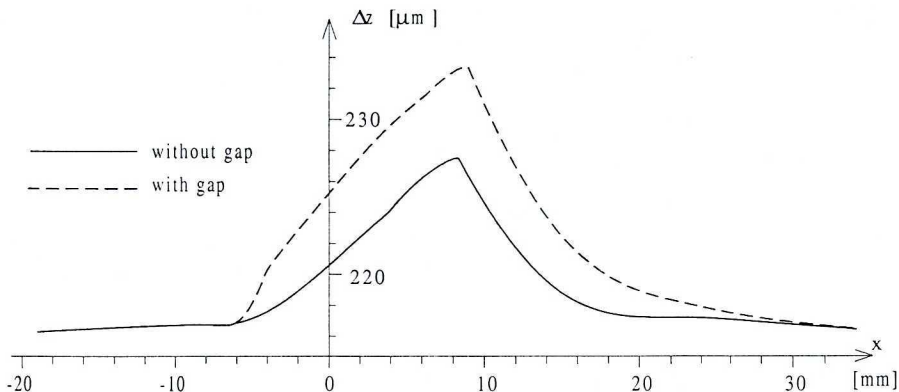


Fig. 5. The vertical displacement of the center of cylinder in domain of the cylinder current position

3. Part II – Dynamic analysis of the bogie motion on the track

In order to determine the possibly realistic dynamic wheel-rail contact forces by means of the computer simulation, it is necessary to introduce an appropriate mechanical model of the railway running gear and the track. This model should enable us to investigate the vehicle-track dynamic interaction in the frequency range at least $0 \div 1000$ Hz, with particular attention focused on the so called medium frequency range of $30 \div 500$ Hz. As it follows from e.g. [7], one can limit the study to a single bogie-track interaction, because in this range of frequency the relatively “soft” vehicle primary and secondary suspension springs yield weak coupling effects between the wheelsets, bogie frame and the car-body. In a contradistinction to similar models applied so far for the low frequency range $0 \div 30$ Hz, for this purpose the wheelset axles, wheels and the track must be regarded as flexible elements. According to the above, for dynamic investigations in the medium frequency range, a discrete-continuous mechanical model is proposed in the paper Fig. 6. In this model, the wheelset axles are represented by axially rigid and torsionally deformable continuous rotating visco-elastic Bernoulli-Euler beams in the form of stepped shafts. The wheels are represented by rigid rings attached to appropriate axle cross-sections by using massless elastic isotropic membranes. These membranes facilitate rotations of the rigid rings around their diameters as well as translations along the wheelset axles. In this way, the proposed model of the wheelset wheel enables us to represent the first eigenvibration modes of the railway wheel in the frequency range $0 \div 1000$ Hz. As it follows from natural vibration analyses of the railway wheels performed e.g. in [8], [9] by means of the 3-D finite element approach, in the above mentioned range of frequency the typical wheel has only

one-nodal diameter eigenform of frequency $80 \div 100$ Hz characterized by rotational displacements of the rim around an arbitrary wheel diameter as well as zero-diameter eigenform of frequency $230 \div 350$ Hz characterized by translational displacements of the rim along the wheelset axle. The next, higher eigenmodes are associated with natural frequencies usually greater than 1000 Hz. The wheelset axles are supported at their ends in vertical, longitudinal and axial direction by means of visco-elastic springs corresponding respectively to the vertical, longitudinal and lateral primary suspensions.

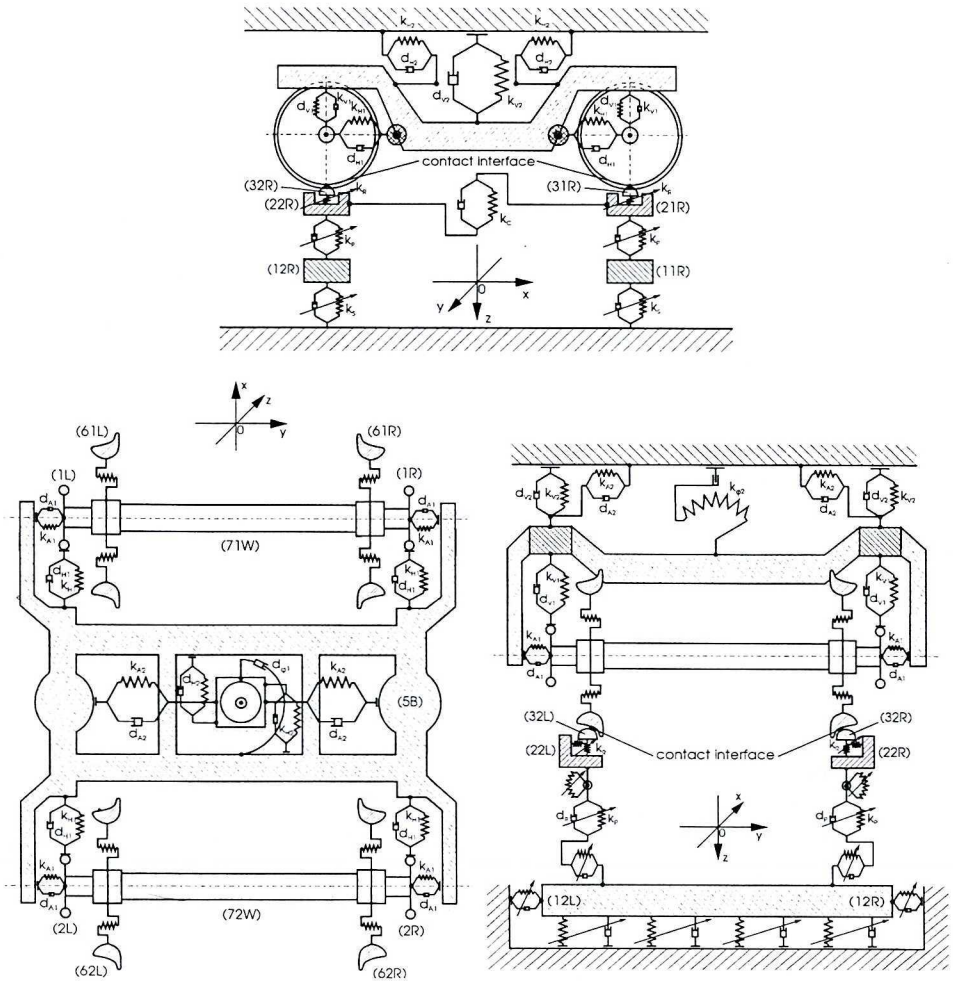


Fig. 6. Discrete-continuous model of the railway bogie-track system

The bogie frame is represented by a rigid body of 6 degrees of freedom connected with the car body of infinite inertia by the visco-elastic springs corresponding to the secondary suspension. The bending-torsional-axial vibrations of both wheelsets are coupled through the wheel-rail contact forces with the vertical and lateral vibrations of the track, which is modelled by means of a dynamic inertial-visco-elastic oscillator of 26 degrees of freedom and of periodically fluctuating parameters, as shown in Fig. 6.

According to appropriate assumptions formulated in [10], [11], the characteristic of the presented track model is that, for instantaneous interaction positions "between the sleeper" and "over the sleeper", the static stiffness values and the dynamic receptance functions are very similar to those obtained from experiments on a real track.

For modeling of the wheel-rail dynamic interface, the Kalker's non-linear contact theory is applied.

The proposed model of the bogie is characterized by well known partial differential equations as equations for flexural and torsional motion of cross-sections of the wheelset axles. These equations are solved with appropriate boundary conditions, which besides of respective geometrical conformity conditions for displacements and inclinations, contain linear and nonlinear equations of equilibrium for the inertial, elastic, contact, gravitational and external damping forces, support reactions, gyroscopic moments as well as for static and dynamic unbalance forces and moments. The equations of boundary conditions contain all the non-linear and parametric terms describing excitation due to contact forces, unbalance effects and interactions with the supports. These equations are coupled with ordinary differential equations with variable coefficients which govern the motion of the track model and the lateral vibrations of the entire bogie. The detailed form of the proposed mathematical model as well as the method of its solving are described in [10], [11]. Solving the differential eigenvalue problem of the linearized system and an application of the Fourier solutions in the form of series lead to the set of modal equations in the Lagrange co-ordinates $r_n(t)$, $n = 1, 2, \dots, \infty$,

$$\mathbf{M}(t) \ddot{\mathbf{r}}(t) + \mathbf{C}(t, \dot{r}_n(t), r_n(t)) \dot{\mathbf{r}}(t) + \mathbf{K}(t, r_n(t)) \mathbf{r}(t) = \mathbf{F}(t, r_n(t)). \quad (2)$$

These equations are coupled by the parametric, non-linear and gyroscopic terms regarded as external excitations expanded in series in the analytical eigenfunctions, the result of which are full mass, damping-gyroscopic and stiffness matrices denoted in (2) as \mathbf{M} , \mathbf{C} and \mathbf{K} , respectively. A fast

convergence of the Fourier solutions applied for the proposed approach enables us to reduce the number of the modal equations that should be solved, in order to obtain a sufficient accuracy of results in the given range of frequency. Such a mathematical description of the investigated bogie-track model is formally strict, demonstrates clearly the qualitative system properties and is very convenient for a stable and efficient numerical simulation.

The numerical calculations were performed for the freight-car two-axle bogie with the wheelbase 1.80 m. There was assumed motion of the bogie with various travelling speeds in the range $v_0 = 40 \div 120$ km/h under the gravitational load 230 kN per axle along the typical straight track of relatively high average vertical stiffness $2.03 \cdot 10^8$ N/m, the rails of which are supported on concrete sleepers. The measured and calculated vertical and lateral dynamic receptances of this track can be found in [10], [11]. The natural track property fluctuation during the run over successive sleepers with the so called “track excitation frequency” equal to v_0/l_s was regarded here as the steady-state excitation source of the parametric type, where $l_s = 0.6$ m denotes the sleeper spacing. In order to focus the investigations on the transient vibrations induced by passage of the bogie along the “squat”-type crack on the rail running surface, the ideal wheel-rail geometry was assumed, i.e. ideally round wheel treads and perfectly even rails. As the only kinematic excitation source the measured rail unevenness caused by the presence of “squat”-type crack was assumed in the form of the presented in Fig. 5 penetration depth history expressed as a function of the wheel current position on the right-hand rail. In order to obtain possibly most severe dynamic response due to this excitation, the “squat”-type crack was assumed to occur on the hardest track section, i.e. in the rail tread section directly over the sleeper, where the position of crack maximal depth was exactly above the sleeper longitudinal symmetry axis. The most interesting calculated quantity was the vertical wheel-rail dynamic contact force caused by the simulated bogie-track interaction.

Figure 7 a, b and c presents the time histories of the wheel-rail dynamic vertical contact force obtained by numerical simulation expressed as functions of the traveled distance with the train speed values respectively 60, 80 and 120 km/h. In this figure, the black lines denote the responses for the right wheel of the first wheelset of the bogie, the grey lines depict the dynamic responses for the right wheel of the second wheelset and the dashed lines denote the respective static gravitational loads. All the obtained responses are characterized by the predominant steady-state component due to periodic fluctuation of track dynamic and static properties during run over successive

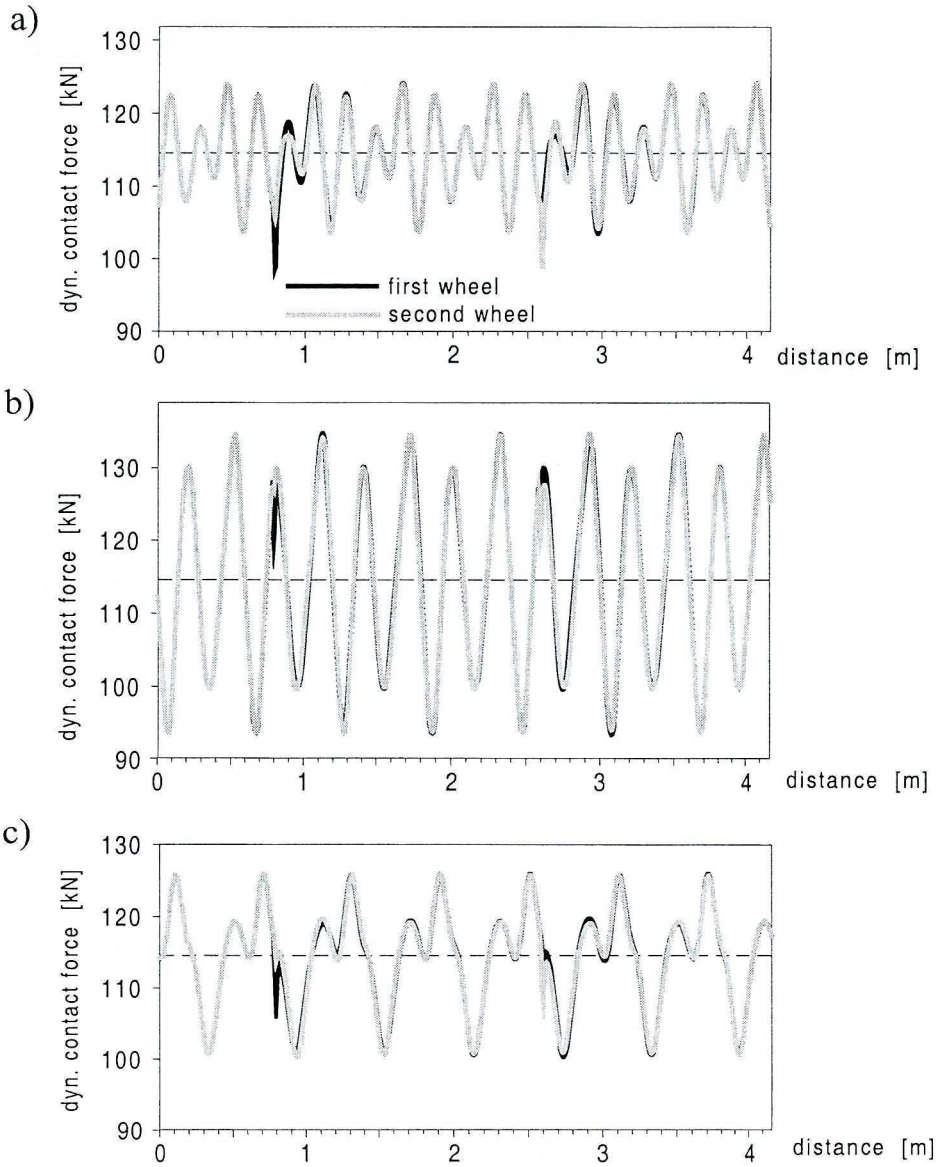


Fig. 7. Wheel-rail dynamic contact forces due to the passage along the "squat"-type crack in the rail for travelling speeds: (a) 60, (b) 80 and (c) 120 km/h

sleepers. In this steady-state process, there is a superimposed transient component excited by the passage of two successive wheels of the bogie along the unevenness caused by the “squat”-type crack, which results in temporary decrease of the contact force in the form of small ‘negative peaks’. Arguments of these peaks correspond to the above-mentioned assumed position of the “squat”-type crack on the rail tread section. It is to emphasize that, for the considered travelling speed values, the absolute values of these ‘peaks’ are smaller than amplitudes of the steady-state response due to the track property fluctuation during the run, Fig. 7. As it follows from the results of all performed simulations, not presented here in the form of graphs, the influence of the passage along the “squat”-type crack in the right-hand rail on the dynamic left-hand wheel-rail vertical contact force is negligible. The authors performed an additional simulation in order to determine the magnitude of the dynamic response of the bogie-track system induced by the passage of the bogie right wheels along the rail unevenness caused by the “squat”-type crack. In this case, the fluctuation of track properties during run over successive sleepers was artificially neglected. The results of this simulation for the bogie travelling speed $v_0 = 60$ km/h are shown in Fig. 8. Here, one obtains the histories of the wheel-rail vertical contact forces for both right-hand bogie wheels in the form of two successive typical transient vibration processes decaying relatively fast with time. The initial amplitudes of these processes are much smaller than the amplitudes of the wheel-rail vertical dynamic contact forces due to the periodic fluctuation of track properties during run over successive sleepers, as it follows from respective plots in Fig. 7a.

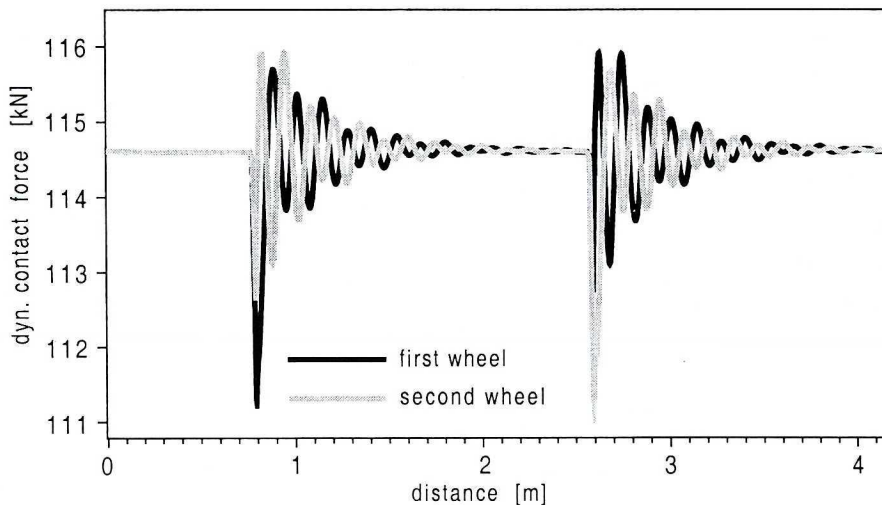


Fig. 8. Transient component of the bogie track dynamic response caused by the rail unevenness of the “squat”-type

Fig. 9 shows the plots of dynamic wheel-rail contact force history in the domain of wheel temporary position, for two travelling speed values at 60 and 120 km/h, when the wheel of the first bogie wheelset passes the crack. In this figure, the plot of variation of stress intensity factor K_{II} for a quasi-static wheel rolling along the crack with a gap under a constant load is also presented.

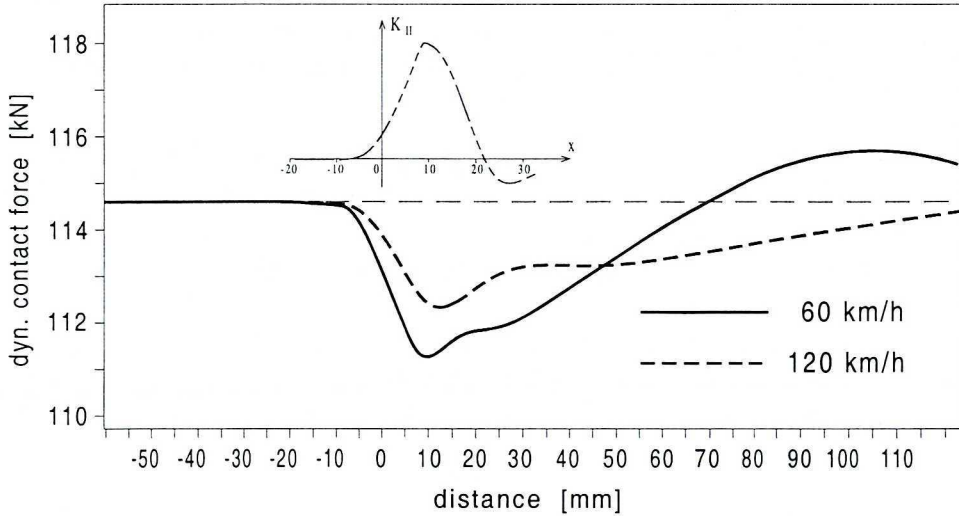


Fig. 9. Dynamic wheel-rail contact force for the first bogie wheelset wheel rolling along the even rail with the kinematic excitation representing a crack in the tread. Stress intensity factor K_{II} for the quasi-static rolling of the cylinder along the cracked prism in the domain of cylinder position

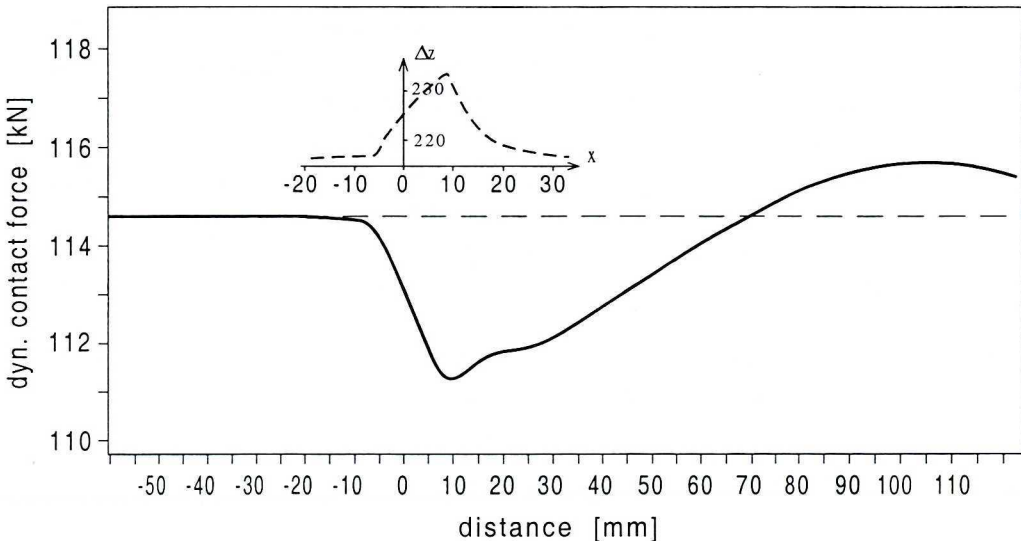


Fig. 10. Dynamic contact force for the first bogie wheelset wheel rolling with the travelling speed 60 km/h along the even rail with the kinematic excitation caused by the crack in the tread demonstrated together with the plot of cylinder vertical displacement expressed as the function of wheel position

It follows from such a demonstration that for wheel positions which cause the greatest changes of K_{II} , the dynamic wheel-rail contact force is smaller than the static one. For the travelling speed 60 km/h, the dynamic contact force exceeds the static value for wheel positions greater than 70 mm from the begin of the crack, but then the wheel-crack interaction is relatively weak and K_{II} tends to zero. For greater travelling speeds, the dynamic contact force exceeds the static force value for wheel even more greater distances from the crack. Thus, with the dynamic processes taken into consideration, the amplitude of ΔK_{II} will be smaller than that determined for the static loads.

It follows from the plot of dynamic wheel-rail contact force demonstrated together with the plot of vertical displacements of the cylinder center that the maximal dynamic force exceeds the static force when the wheel leaves the tread area where the influence of the crack on the vertical wheel displacement is remarkable, Fig. 10.

Such a history of the dynamic contact force during the wheel passage over the “squat”-type crack is caused by the transient vertical vibration component induced by the kinematic excitation according to the existence of rail tread unevenness.

4. Conclusions

The expectations that during railway bogie wheelset wheel passage along the rail with the “squat”-type crack in its tread is a source of the dynamic wheel-rail contact forces provoking faster crack development have not been confirmed. For the wheel positions, which cause the greatest changes of K_{II} , the value of dynamic contact force surplus is negative. However, if this dynamic force surplus is positive, the wheel runs in the meantime so far away from the crack position that its influence on the crack area seems to be negligible. Then, one can disregard the dynamic effects induced by the cracked rail tread, because these effects result in decreasing of the amplitude ΔK_{II} . The performed analysis leads to the conclusion that the dynamic contact force surplus resulting from the support of rails on sleepers should be taken into consideration. It is obtainable by increasing the normal load Q , Fig. 3, because the oscillation wave of the dynamic contact force is much longer than the rail section along which the crack can influence the vertical displacements of the railway wheel.

This work has been financially supported by the Polish Research Council (KBN) – Project No 7 T07A 43 15.

Manuscript received by Editorial Board, January 22, 2003;
final version, June 12, 2003.

REFERENCES

- [1] Bogdański S., Olzak M., Stupnicki J.: Influence of liquid interaction on propagation on rail rolling contact fatigue cracks., Proc. 2nd Mini Con. on Contact Mechanics and Wear of Rail/Wheel Systems, Budapest 29-31 July 1996, pp. 134 + 143.
- [2] Bogdański S., Olzak M., Stupnicki J.: The effect of face friction and tractive force on propagation of 3D 'squat' type of rolling contact fatigue crack., Proc. 2nd Mini Con. on Contact Mechanics and Wear of Rail/Wheel Systems, Budapest 29-31 July 1996, pp. 164 + 173.
- [3] Olzak M., Stupnicki J.: Zmienność współczynników intensywności naprężenia w trakcie przetaczania obciążenia po bieżni ze szczeliną; Część I: Szczeliny o niegładkich powierzchniach, VII Krajowa Konferencja Mechaniki Pęknięcia, Kielce-Cedzyna 23-25 września 1999, pp. 109 + 116.
- [4] Olzak M., Stupnicki J.: Zmienność współczynników intensywności naprężenia w trakcie przetaczania obciążenia po bieżni ze szczeliną; Część II: Szczeliny z luzem oraz warstwami materiału o zmienionych właściwościach, VII Krajowa Konferencja Mechaniki Pęknięcia, Kielce-Cedzyna 23-25 września 1999, pp. 109 + 116.
- [5] Bogdański S., Olzak M., Stupnicki J.: Numerical modeling of a 3D rail RCF 'squat'-type crack under operating load, Fatigue & Fracture of Engineering Materials & Structures 1998; 21, pp. 923 + 935.
- [6] Olzak M., Stupnicki J., Wójcik R.: Numerical Analysis of surface crack propagation in rail-wheel contact zone, Proc. of the Int. Conf on "Rail Quality and Maintenance for Modern Railway Operation", Delft, June 1992, pp. 385 + 395.
- [7] Popp, K. - Kruse, H. - Kaiser, I.: Vehicle-track dynamics in the mid-frequency range, Vehicle System Dynamics, Vol. 31, No. 5-6, 1999, pp. 423 + 464.
- [8] Fingberg U.: Ein Modell für das Kurvenquietschen von Schienenfahrzeugen, VDI Fortschritt-Berichte, Reihe 11, Nr. 140, 1990.
- [9] Meinders T., Meinke P.: Rotor dynamics and irregular wear of elastic wheelsets, Karl Popp & Werner Schiehlen (Eds.) "System Dynamics and Long-Term Behaviour of Railway Vehicles, Track and Subgrade", Springer-Verlag, 2002, pp. 133 + 152.
- [10] Szolc T.: On discrete-continuous modelling of the railway bogie and the track for the medium frequency dynamic analysis, Engineering Transactions, No. 48, 2, 2000, pp. 153 + 198.
- [11] Szolc T.: Simulation of dynamic interaction between the railway bogie and the track in the medium frequency range, Multibody System Dynamics, 6, 2001, pp. 99 + 122.

Efekty dynamiczne powodowane przez pęknięcie typu "squat" w bieżni szyny kolejowej

S t r e s z c z e n i e

Prezentowany materiał jest częścią prac mających na celu wyjaśnienie mechanizmu rozwoju pęknięć typu "squat" pojawiających się w bieżniach szyn kolejowych. W tym artykule autorzy

przedstawiają badania nad ustaleniem wpływu jaki na rozwój pęknięcia tego typu mogą mieć obciążenia dynamiczne występujące w systemie składającym się z prostego odcinka toru kolejowego i poruszającego się po nim obciążonego wózka przy czym w jednej z szyn założono obecność pęknięcia "squat".

Badania prowadzono metodami symulacji numerycznych. Badania te były podzielone na dwa etapy. W pierwszym ustalono jak w trakcie quasi-statycznego przetaczania koła po szynie z pęknięciem zmienia się sztywność układu koło-szyna. W drugim zmiany sztywności układu koło-szyna uwzględniono w analizie dynamiki ruchu wózka po torze. W wyniku analizy dynamicznej uzyskano wykresy obrazujące zmiany sił nacisku kół na szyny z uwzględnieniem obecności pęknięcia.